Double-Layered Electrospun Nanofiber Filter for the Simultaneous Removal of Urea and Ammonium from Blood

Makoto Sasaki [a,b], *László Szabó* [a]†, *Koichiro Uto* [a], *and Mitsuhiro Ebara** [a, b]

a. Research Center for Macromolecules and Biomaterials, National Institute for Materials Science (NIMS), 1-1 Namiki, Tsukuba, Ibaraki, 305-0044 Japan

b. Graduate School of Pure and Applied Sciences, University of Tsukuba, 1-1-1 Tennodai, Tsukuba, Ibaraki, 305-8571 Japan

KEYWORDS: Nanofibers, wearable artificial kidney, urease, electrospinning, chitosan

ABSTRACT

A major challenge in the development of wearable artificial kidneys lies in the efficient removal of urea, which is found at an extremely high concentration in the blood of patients with chronic kidney disease (CKD). Urease is an enzyme that hydrolyzes urea. While it can efficiently remove urea, toxic ammonium is produced as a byproduct. In this study, nanofibers capable of removing both urea and ammonium from blood were fabricated. Specifically, urease was immobilized on electrospun poly(ethylene-*co*-vinyl alcohol) (EVOH)/chitosan nanofiber membranes via covalent crosslinking. Chitosan not only helped covalent immobilization via its free amino groups, but also improved hemocompatibility by suppressing protein adhesion. The resulting urease-immobilized EVOH/chitosan nanofibers exhibited an outstanding urea removal performance of 690 mg/g per hour. For ammonium removal, EVOH nanofiber membranes containing sodium cobalt(II) hexacyanoferrate(II) (NaCoHCF), an ammonium adsorbent, were prepared. The fabricated EVOH/NaCoHCF membranes exhibited an ammonium adsorption capacity of 135.5 mg/g. The two types of nanofiber membranes were combined to form a double-layered nanofiber membrane that was placed in a filter holder for continuous-flow cycling experiments. Under such conditions, all urea at a concentration similar to that in the blood of CKD patients was degraded within 1 hour, and ammonium production was reduced by approximately 90% of the normal level. This double-layered nanofiber membrane is a novel material that can achieve both urea degradation and ammonium adsorption, and is expected to advance the development of wearable artificial kidneys, a game-changer in the treatment of CKD.

1. Introduction

In healthy individuals, waste products in the blood are filtered by the kidneys and excreted from the body as urine. However, patients with dysfunctional kidneys have chronic kidney disease (CKD). Under such pathological conditions, waste products accumulate in the blood, causing various complications.[1] The only intervention that can fundamentally cure CKD is kidney transplantation; however, the shortage of donors and severe rejection after transplantation limit its applicability as a universal treatment option.[2–4] Therefore, hemodialysis is the most commonly used method to treat CKD. Nevertheless, hemodialysis is extremely burdensome to the patient, as it requires three visits per week and approximately 4 hours of treatment each time. In addition, as hemodialysis requires a large amount of water, it is difficult to perform in developing countries or during disasters, when water is scarce.[5] To resolve this problem, various research groups have developed wearable artificial kidneys (WAK). The first WAK was introduced in 1976 by Dr. Willem Kolff, who developed hemodialysis.[6] This WAK used charcoal to remove waste products from the dialysate solution, making the solution reusable, thereby reducing the amount of water required for treatment and decreasing the device size. Ever since, several other WAK have been developed;[7–10] yet none of them are widely used because of their inadequate urea removal performance.

Urea is a typical uremic toxin that accumulates in the blood of patients suffering from CKD at a very high concentration (230 mg/dL).[11] Urea is found at the highest concentration among approximately 100 substances reported as uremic toxins. Recently, urea has also been reported to be a toxin that should be removed from blood, because it is found to act on vascular endothelial cells and promote the production of reactive oxygen species.[12,13] However, owing to its small size (low molecular weight) and charge neutrality, urea is extremely difficult to remove via adsorption.[14] Although many researchers have attempted to develop urea adsorbents, the

adsorption performance of the developed materials has been inadequate, thus, a large amount of adsorbent is required to completely remove the urea present in blood.[15–19]

Another effective approach for urea removal is its degradation. Urease is an enzyme that hydrolyzes urea, and many materials have been developed to immobilize it.[20–25] These materials have superior urea removal performance compared to adsorption methods, but ammonium, which is also known to be highly toxic in the blood, is produced as a byproduct of urea degradation, which is a major obstacle to the practical use of WAK.

In this study, we designed and developed a new material to simultaneously solve the two conventional problems of removing urea from blood: "low adsorption performance" and " ammonium production." Specifically, we fabricated double-layered nanofibers composed of the layer for urea degradation and the layer for ammonium removal. The first layer is composed of poly(ethylene-*co*-vinyl alcohol) (EVOH) and chitosan nanofibers via electrospinning (Figure 1). EVOH is not only highly linear and suitable for electrospinning, but exerts hemocompatibility, and therefore, it has already been used in hemodialysis membranes.[26] Chitosan, a polysaccharide with highly reactive amino groups, was used to immobilize urease on the nanofibers. As a natural polysaccharide derived from crustacean shells, chitosan has attracted significant attention in recent years because of its ability to be chemically modified using its amino and hydroxyl groups.[27,28] Subsequently, we immobilized urease on the first layer of the double-layered nanofibers using glutaraldehyde as a crosslinking agent to form chemical bonds between the amino groups of chitosan and urease. It should be noted that chitosan not only helped immobilize urease, but also greatly suppressed protein adsorption, improving the hemocompatibility of the membrane. Further, we incorporated sodium cobalt(II) hexacyanoferrate(II) (NaCoHCF) as an ammonium adsorbent in the second layer. This allowed both urea degradation and ammonium

adsorption to be achieved using a single material. NaCoHCF is a Prussian blue-type complex that has been reported to exhibit high adsorption performance and selectivity for ammonium ions through ion-exchange reactions.[29] Nevertheless, if NaCoHCF is used directly, there is a risk of toxicity due to direct contact with the blood or leakage of NaCoHCF into the blood. To prevent this, EVOH nanofibers containing NaCoHCF were prepared and used as ammonium adsorption filters. The nanofibers were fabricated by electrospinning, a typical nanofiber fabrication method.[30]

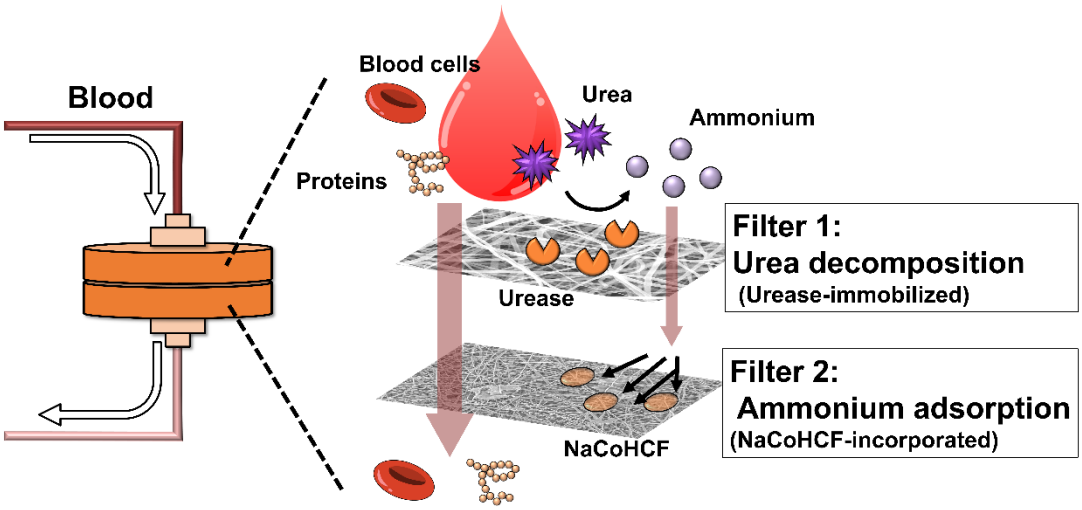

Figure 1. Schematic of urea removal from blood using double-layered nanofibers.

2. Materials and Methods

2. 1. Materials

An EVOH copolymer (EVAL® E105A) with 44 mol% ethylene ratio was purchased from Kuraray Co., Ltd (Tokyo, Japan). Another EVOH copolymer (Soarnol™ V2504RB) with 25 mol% ethylene ratio was purchased from Mitsubishi Chemical Corporation (Tokyo, Japan). Low-molecular-weight chitosan (Catalog Number 448869) was purchased from Sigma-Aldrich (USA). 1,1,1,3,3,3-Hexafluoro-2-propanol (HFIP) was purchased from Tokyo Chemical Industry

Co., Ltd. (Tokyo, Japan). Dulbecco's phosphate-buffered saline (PBS) and human serum albumin (HSA) were purchased from Nacalai Tesque Inc. (Kyoto, Japan). Acetic acid, 25% aqueous glutaraldehyde solution, urease, urea, sodium ferrocyanide decahydrate, cobalt(II) nitrate hexahydrate, ammonium chloride, sodium dodecyl sulfate (SDS), and sodium hydroxide were purchased from FUJIFILM Wako Pure Chemical Corporation (Osaka, Japan). The urea assay kit was purchased from Cosmo Bio Co., Ltd. (Tokyo, Japan). Porcine blood samples were purchased from Tokyo Shibaura Zouki (Tokyo, Japan). Micro BCA™ Protein Assay Kit was purchased from Thermo Fisher Scientific K.K. (Tokyo, Japan).

2.2 Preparation of EVOH/chitosan nanofibers

First, EVOH and chitosan solutions were prepared separately. EVOH with an ethylene ratio of 44 mol% was dissolved in HFIP at 4 wt% concentration via sonication. Chitosan was dissolved in a mixed solvent consisting of acetic acid, distilled water, and HFIP (45:5:50 wt%) at 2 wt% concentration by stirring overnight, followed by centrifugation to remove the undissolved material. The chitosan and EVOH solutions were mixed at predetermined ratios to obtain electrospinning solutions with final chitosan concentrations of 0.4, 0.5, 0.7, 1.0, and 1.6 wt%. The detailed mixing ratios are listed in Table 1. The viscosity of these solutions was measured to check the spinnability for electrospinning. The solution was injected into a viscometer (RheoSense *micro*VISC-m) at room temperature, and viscosity was calculated using the mixed solvent consisting of acetic acid, distilled water, and HFIP as a reference. Finally, the mixed electrospinning solution was electrospun on ESM-101 (MECC Co., Ltd., Fukuoka, Japan) using a 22 G needle at 30 kV applied voltage and 1.0 mL/h feeding rate. The collector-to-needle distance was 15 cm.

2.3 Synthesis of NaCoHCF

NaCoHCF was synthesized in accordance with a previous report. Sodium ferrocyanide decahydrate and cobalt(II) nitrate hexahydrate were dissolved separately in ultrapure water to prepare 0.4 mol/L solutions.[29] The two solutions were mixed in a beaker and stirred at room temperature for 15 min to obtain a slurry. The slurry was then washed five times via centrifugation by replacing the supernatant with fresh water each time. Then, the slurry was lyophilized overnight to obtain NaCoHCF as a powder.

2.4 Preparation of EVOH/NaCoHCF nanofibers

EVOH with an ethylene ratio of 25 mol% was dissolved in HFIP at a concentration of 4 wt% via sonication. Then, the NaCoHCF powder was added to the EVOH solution at 10, 20, 30, 40, 50, and 60 wt% of the polymer content and dispersed via sonication. The resulting mixture was electrospun using an 18G needle at 25 kV, 1.0 mL/h feeding rate, and 15 cm distance between the needle and collector.

2.5 Characterization of nanofibers

Field-emission scanning electron microscopy (FE-SEM; Hitachi SU8230) was performed to observe the morphology of the fabricated nanofibers and analyze the atoms by energy dispersive X-ray spectroscopy (EDX). Before observation, the dried samples were placed on a sample stage and coated with Pt. The average fiber diameter was calculated by measuring the diameters of at least 30 fibers using the ImageJ software.

Fourier transform infrared (FT-IR) spectra were recorded in the absorbance mode (Shimadzu IRAffinity-1S) with 64 scans and a resolution of 4 cm^{-1}. The spectra were obtained in the 300 to 7900 cm^{-1} range, but only the range necessary for analysis is shown in the manuscript.

Thermogravimetric analysis (TGA; Seiko Instruments TG/DTA6200) was performed to determine the chitosan content in the EVOH/chitosan nanofibers and the NaCoHCF content in the EVOH/NaCoHCF nanofibers. The nanofiber or powder samples were loaded into an alumina pan, and the temperature was increased from 25 °C to 550 °C with 10 °C/min heating rate under nitrogen flow. The temperature was maintained at 550 °C for 10 min to allow the reaction to proceed completely.

The surface wettability of EVOH and EVOH/chitosan nanofibers was evaluated by measuring the water contact angle in air using an automatic contact angle meter (Kyowa Interface Science DM-700, Kyoto, Japan). 1 μL droplet of water was applied to the nanofibers fixed on a glass slide. Because the EVOH/chitosan nanofibers quickly absorbed water, the contact angle was measured every second for 5 s after the drop was applied.

X-ray diffraction (XRD) measurements were performed to investigate the crystal structures of NaCoHCF and the EVOH/NaCoHCF nanofibers before and after ammonium adsorption. XRD patterns were obtained using an X-ray diffractometer (Rigaku SmartLab) by the $2\theta/\theta$ method, with a slit width of 5 mm, a measurement angle of 5 to 60°, and a measurement interval of 0.02°. A scan speed of 5°/min was used for powders and 0.5°/min for nanofibers.

2.6 Protein adsorption test for hemocompatibility evaluation

The experiment was conducted in accordance with a previous report.[31] The prepared nanofiber sheets were cut into 5 mm diameter circles and placed individually in the wells of a 96-well plate.

After being washed five times with PBS, 150 μL of 5% SDS/0.1 N NaOH solution was added to each well, and the wells were incubated at 37 °C for 1 h to remove the adsorbed HSA. The amount of HSA adsorbed to the nanofibers was calculated by measuring the concentration of HSA in the supernatant with the Bicinchoninic Acid Assay (BCA).

2.7 Immobilization of urease on EVOH/chitosan nanofibers

EVOH/chitosan nanofibers (10 mg) were immersed in 20 mL of a 2% glutaraldehyde solution to enable the reaction of glutaraldehyde with the amino groups of chitosan. After standing at room temperature for 30 min, the nanofibers were washed three times with distilled water to remove the unreacted glutaraldehyde. The nanofibers were then immersed in 20 mL of a 2% urease solution to react with the amino groups of urease. After being stood at room temperature for 30 min, the nanofibers were washed three times with distilled water to remove excess urease.

2.8 Urea degradation test

Urea degradation tests were performed using PBS or porcine blood samples. Urea was dissolved in PBS or porcine blood at 230 mg/dL, which is equal to the blood concentration in patients with CKD (as the highest mean/median uremic concentration based on the literature report).[11] The nanofibers were immersed in 3 mL of this solution and shaken at 37 °C in a thermostatic shaking chamber, and 100 μL of the supernatant was collected at a predetermined time. The supernatant was diluted 5-fold with PBS or porcine blood to obtain a sample with a urea concentration that matched the measurement range of the assay kit. The solution was colored by the reagent in the assay kit (BioChain Institute Urea Assay Kit) and allowed to stand at room temperature for 20 min, and the urea concentration was determined by measuring the

absorbance at 520 nm (using a Tecan Infinite M Nano+ microplate reader). The urea concentration in the original solution was calculated by multiplying the determined concentration by 5 (dilution ratio).

2.9 Ammonium adsorption test

Ammonium chloride was dissolved in PBS to prepare a 1.0 g/L ammonium solution. Then, 50 mg of the NaCoHCF powder or EVOH/NaCoHCF nanofibers was added to 20 mL of the ammonium solution and shaken at 37 °C using a constant-temperature shaking chamber. At a predetermined time, 1 mL of the supernatant was collected and diluted 10-fold with PBS to prepare a measurement solution. In the case of the NaCoHCF-based sample, the solid powder was removed via centrifugation at 3500 rpm for 3 min, and the supernatant was collected. The ammonium concentration in the solution was measured using an ammonia analyzer (Toko Kagaku TiN-9001), according to the manual of the ammonia-measuring instrument. The ammonium concentration in the original solution was calculated by multiplying the measured concentration by 10. The ammonium adsorption capacity of the sample was calculated using equation (1):

$$Ammonium\ adsorption\ capacity\ = (C_0 - C_1) \times V/W \qquad (1)$$

where C_0 and C_1 are the initial and final concentrations of urea solution respectively, V is the volume of urea solution, and W is the weight of the NaCoHCF.

2.10 Fabrication and evaluation of double-layered nanofibers

Double-layered nanofibers were fabricated via sequential electrospinning steps. First, 5 mL of the EVOH/NaCoHCF solution was spun to produce EVOH/NaCoHCF nanofibers, according to the procedure described in Section 2.4. Then, EVOH/chitosan nanofibers were spun on top of the EVOH/NaCoHCF nanofibers using 1 mL of the EVOH/chitosan solution, according to the procedure described in Section 2.2.

Double-layered nanofibers were evaluated using FE-SEM and urea degradation tests. Urease was immobilized on the nanofibers using the procedure described in Section 2.7. Then, the nanofibers were placed in a filter holder (Merck Millipore Swinnex Filter Holder, 47 mm) and connected to a tube (Fuji Systems Phycon tube SH No. 4), diaphragm pump (KNF FF12 DC-M), and DC power supply (CUSTOM DPS-3005). A 230 mg/dL urea solution was prepared in PBS, and 30 mL of the urea solution was circulated through the double-layered nanofibers while being warmed to 37 °C, and the filtered solution was collected at predetermined times. The flow rate was set at 100 mL/min. The urea and ammonium concentrations of the collected solutions were measured using the methods described in Section 2.8 and 2.9, respectively, and the changes in the concentration of each were evaluated.

3. Results and Discussion

3.1 Fabrication of EVOH/chitosan nanofibers

To develop a material for removing both urea and its degradation byproduct, ammonium ions, from blood, we fabricated EVOH/chitosan nanofiber membranes as substrates for the immobilization of urease. However, the fabrication of polymer nanofibers incorporated with chitosan by electrospinning has been reported to be extremely difficult.[32] One reason is that the chitosan solution has a very high viscosity due to its polycationic properties and strong

intermolecular hydrogen bonds. Therefore, we first focused on preparing a chitosan solution with a viscosity suitable for electrospinning to fabricate nanofibers. We prepared mixtures of acetic acid, water, and HFIP at various ratios and examined the solubility of chitosan in the mixtures. We found that a mixture with acetic acid:water:HFIP weight ratio of 45:5:50 dissolved chitosan adequately. To prepare electrospinning solutions, a 2 wt% chitosan solution prepared using this solvent mixture was mixed with a 4 wt% EVOH solution at different ratios. The mixing ratios and final chitosan concentrations are listed in Table 1. The effect of the chitosan concentration on the solution viscosity is shown in Figure 2a. One reason for difficulty of electrospinning chitosan is that the viscosity of the solution is either too low or too high, making it difficult to handle. [33] The maximum viscosity of the prepared EVOH/chitosan solution was 320.1 mPa-s, which is within the appropriate range. Therefore, this solution was used to produce nanofibers by electrospinning.

Table 1. Ratios of EVOH and chitosan solutions used for preparing electrospinning solutions

4 wt% EVOH solution (g)	**2 wt% chitosan solution (g)**	**Final EVOH concentration (wt%)**	**Final chitosan concentration (wt%)**
4	1	3.2	0.4
3	1	3.0	0.5
2	1	2.7	0.7
2	2	2.0	1.0
1	4	0.8	1.6

The FE-SEM images of the nanofibers electrospun using these solutions are shown in Figure 2c–h. Nanofibers with a uniform structure were obtained at chitosan concentrations of 0.4, 0.5, and 0.7 wt%, while the formation of bead-like structures was observed at 1.0 wt% chitosan loading. Beaded structures are generally undesirable, because they impair the uniformity of the nanofibers. Bead structures are known to form when the polymer concentration in the solution is insufficient, limiting the entanglement of the polymer chains.[34,35] In the EVOH/chitosan nanofibers, EVOH is considered to be the main fiber-forming component. As the ratio of chitosan in the electrospinning solution increases, that of EVOH decreases proportionally, which may be the reason for the formation of a beaded structure. When the chitosan concentration was increased to 1.6 wt%, no nanofiber formation was observed. The average diameter of the nanofibers, measured using ImageJ software, was found to decrease with increasing chitosan concentration (Figure 2b). The decrease in EVOH concentration in the solution may have caused these phenomena as well. Because a higher concentration of chitosan in the nanofibers is desirable to immobilize more urease, EVOH/chitosan nanofibers prepared using a solution with 0.7 wt% chitosan, which is the highest concentration at which bead structure formation was not observed, were used in subsequent experiments.

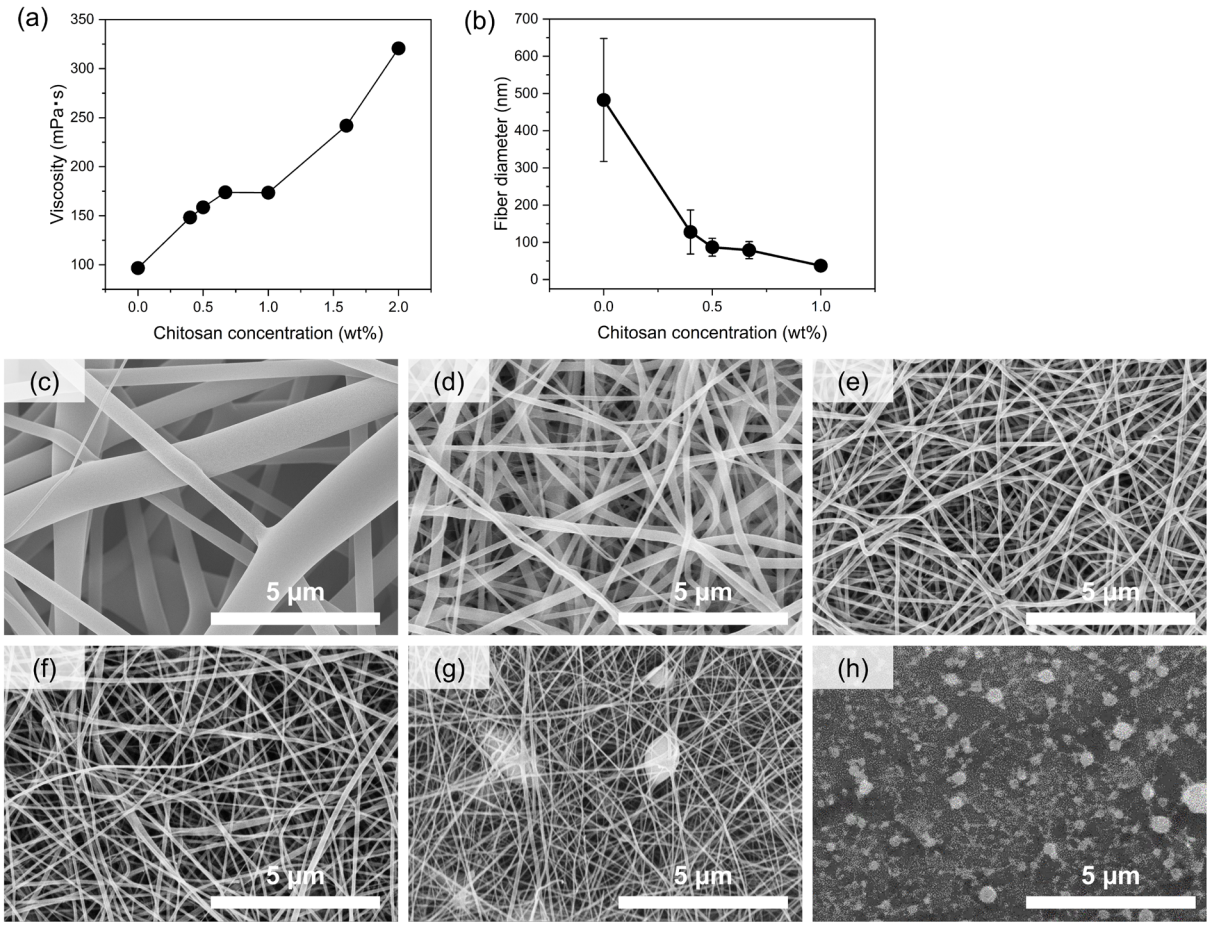

Figure 2. (a) Viscosities of the EVOH/chitosan solutions used for electrospinning. (b) Diameter of the electrospun EVOH/chitosan nanofibers as a function of chitosan concentration. (c-h): FE-SEM images of electrospun EVOH/chitosan nanofibers. Chitosan concentration in the electrospinning solution was varied as (c) 0, (d) 0.4, (e) 0.5, (f) 0.7, (g) 1.0, and (h) 1.6 wt%.

3.2 Synthesis of NaCoHCF and fabrication of EVOH/NaCoHCF nanofibers

NaCoHCF was used as the ammonium adsorbent to remove the ammonium produced by urea degradation. The FE-SEM images of NaCoHCF, synthesized according to a previously reported method[29], are shown in Figure 3a. The average particle size was 9.0 ± 4 μm. The XRD pattern of the NaCoHCF powder in Figure S1 shows the strong peaks at 17.2°, 24.2°, and 34.8°. The

position of these peaks are same as that reported previously, confirming the successful synthesis of NaCoHCF.[29]

The FE-SEM images of the EVOH/NaCoHCF nanofibers produced by electrospinning are shown in Figure 3b–h. The micron-sized objects observed in the images appear to be NaCoHCF. The surface of NaCoHCF is smooth in Figure 3c–g. This may be because the NaCoHCF particle surface was covered by EVOH. However, in the EVOH/NaCoHCF nanofibers with a NaCoHCF content of 60 wt%, NaCoHCF has a rough surface (Figure 3h). This is thought to be due to the aggregation of NaCoHCF during electrospinning with increasing NaCoHCF content in the electrospinning solution, which impedes coverage with EVOH. This consideration was further supported by the results of the fiber diameter analysis. As shown in Figure 3i, the diameters of the EVOH/NaCoHCF nanofibers prepared using solutions with 10 to 50 wt% NaCoHCF content were smaller than that of pristine EVOH nanofibers, and the fiber diameter was almost the same at approximately 200 nm regardless of the NaCoHCF loading. A similar trend was observed in a previous study in which EVOH/zeolite nanofibers were fabricated.[36] However, the fiber diameter of electrospun EVOH/NaCoHCF increased to 480 nm when the NaCoHCF content was 60 wt%. This result suggests that the EVOH previously consumed to cover NaCoHCF participated in nanofiber formation, because the surface of NaCoHCF was no longer covered with it. If the surface of the NaCoHCF particles is not covered, there is a risk of NaCoHCF leakage from the nanofibers into the blood and the development of hemotoxicity due to direct contact with the blood. Therefore, it is desirable that the surface of NaCoHCF is covered by EVOH. However, to maximize the ammonium adsorption performance of the nanofibers, a higher NaCoHCF content is desirable. For these reasons, the EVOH/NaCoHCF nanofibers with a content of 50 wt% were selected for subsequent studies.

To check the content of NaCoHCF, energy dispersive X-ray spectroscopy (EDX) was performed, and the images of element mapping were shown in Figure S2. From Figure S2b and Figure S2c, it was confirmed that NaCoHCF powder has no carbon atoms but iron atoms. In Figure S2f, a peak of iron atoms was detected from the large object in the middle. This is thought to be derived from NaCoHCF, confirming that EVOH/NaCoHCF nanofibers contain NaCoHCF. On the other hand, in Figure S2e, carbon atoms were detected throughout the nanofibers. Since NaCoHCF has no carbon atoms, the carbon atoms detected were considered to be derived from EVOH. This confirms that the surface of NaCoHCF is covered by EVOH, which is expected to inhibit NaCoHCF leakage.

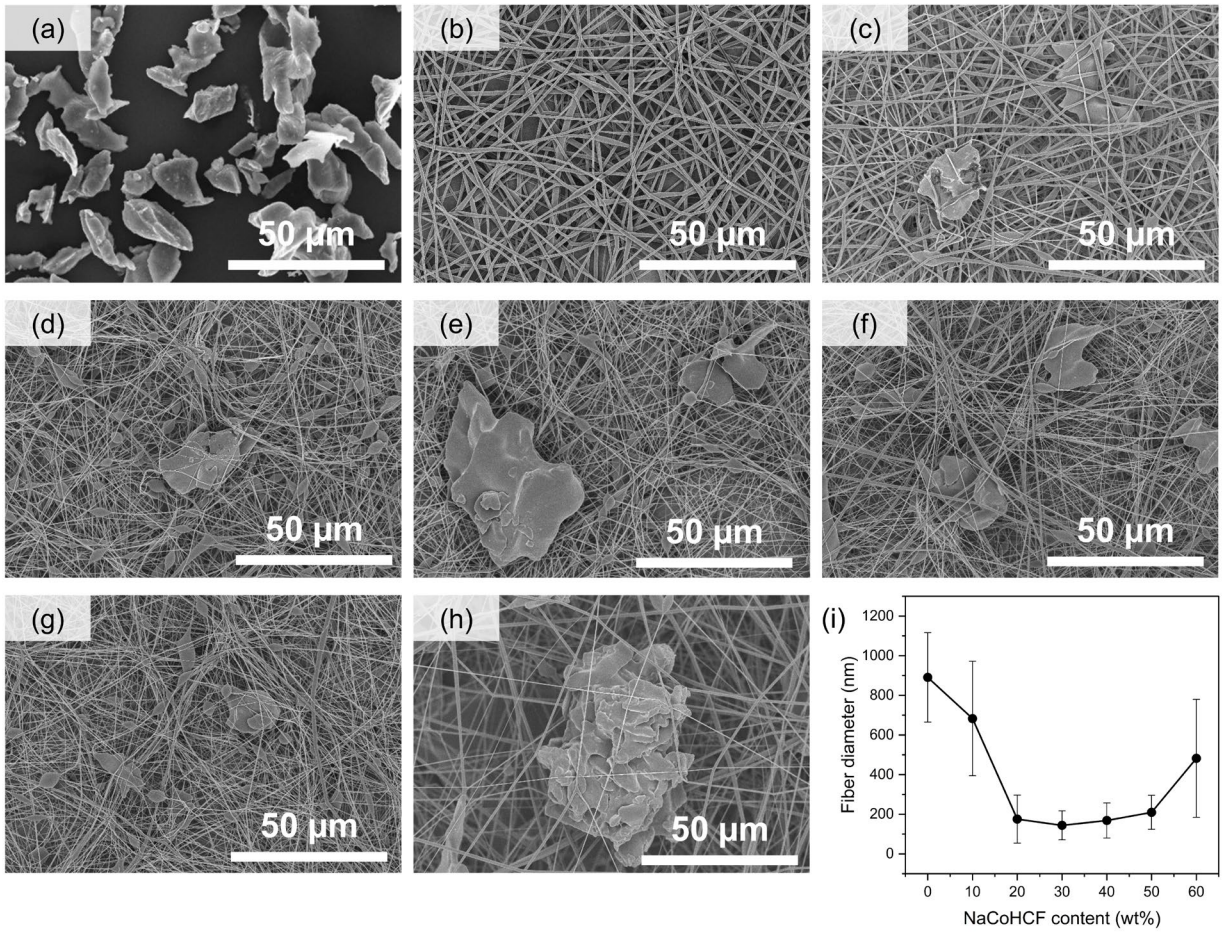

Figure 3. (a) SEM image of the synthesized NaCoHCF powder. (b-h) SEM images of the electrospun EVOH/NaCoHCF nanofibers (NaCoHCF content in the electrospinning solution was (b) 0, (c) 10, (d) 20, (e) 30, (f) 40, (g) 50, and (h) 60 wt%, respectively). (i) Diameter of electrospun EVOH/NaCoHCF nanofibers as a function of NaCoHCF content.

3.3 Characterization of EVOH/chitosan nanofibers

To confirm the presence of chitosan in the EVOH/chitosan nanofibers, the FT-IR spectra of chitosan, EVOH nanofibers, and EVOH/chitosan nanofibers were compared (Figure 4a). For EVOH, peaks at 2928 and 2866 cm^{-1} due to the stretching vibrations of C-H bonds as well as peaks at 1435 and 1339 cm^{-1} due to angular C-H vibrations were observed.[37] Chitosan-derived peaks were observed at 1651 cm^{-1} (stretching of C=O), 1026 cm^{-1} (stretching of C-O), 1373 cm^{-1} (symmetric deformation of -CH_3), and 3000-3600 cm^{-1} (stretching of N-H and O-H).[38] The characteristic peaks of both EVOH and chitosan were observed for EVOH/chitosan nanofibers, confirming the presence of the two materials in the nanofibers.

The TGA curves of chitosan, EVOH nanofibers, and EVOH/chitosan nanofibers are shown in Figure 4b. A weight loss of ~5% was observed between 50 and 100 °C for the chitosan powder. This is due to the evaporation of the water content. Subsequently, a significant mass loss was observed from ~250 °C onwards, probably due to the thermal decomposition of chitosan, and the final residual mass was 38.8% at 500 °C.[38] The EVOH nanofibers also showed a weight loss of ~3% up to a temperature of 100 °C, but their weight remained stable between 100 and ~350 °C. Thereafter, a significant mass loss due to thermal decomposition started around 350 °C, which is 100 °C higher than that of chitosan. The final residual weight was 2.40%.

The EVOH/chitosan nanofibers exhibited a weight loss attributable to the decomposition of chitosan around 250 °C and another weight loss around 350 °C, which can be attributed to the decomposition of EVOH. The TGA curves of three different EVOH/chitosan nanofiber samples fabricated using different chitosan concentrations (0.4, 0.5, and 0.7 wt%) in the electrospinning solution revealed that the residual weights at 500 °C were 1.12, 3.50, and 7.14%, respectively, indicating that the residual weight increased with the chitosan concentration. The chitosan content in the nanofibers was calculated by the following equation (2):

$$Content\ of\ chitosan\ in\ the\ nanofibers\ = W_{nanofibers} \times 100/W_{chitosan} \quad (2)$$

where $W_{nanofibers}$ is the residual weight of each EVOH/chitosan nanofibers at 550 °C, and $W_{chitosan}$ is the residual weight of chitosan powder at 500 °C, which is 38.8 wt%. The calculated contents of chitosan were 2.89, 9.02, and 18.4 wt%, respectively. These samples were rounded to one decimal place and denoted as EVOH/chitosan-3, EVOH/chitosan-9, and EVOH/chitosan-18, respectively. These results confirmed that both EVOH and chitosan were present in the EVOH/chitosan nanofibers and that the chitosan concentration in the nanofibers increased as its concentration in the electrospinning solution increased.

3.4 Characterization of EVOH/NaCoHCF nanofibers

The presence of NaCoHCF in the EVOH/NaCoHCF nanofibers was also confirmed via TGA (Figure 4c). The residual weight of the NaCoHCF powder was 59.9 wt% at 550 °C whereas that of the pristine EVOH nanofibers (without NaCoHCF) was only 2.0 wt%. The weight loss of the NaCoHCF powder below 250 °C is due to the evaporation of water present in it, while the

weight loss that began around 350 °C is due to the thermal decomposition of the material itself.[39] The TGA curve of the EVOH/NaCoHCF nanofibers, shown in orange, shows a weight loss in the 80–200 °C range, similar to that of the NaCoHCF powder, which can be attributed to the evaporation of the internal water of NaCoHCF. The weight loss beginning around 250 °C might be due to the thermal decomposition of EVOH in the EVOH/NaCoHCF nanofibers, and this temperature is ~100 °C lower than that of pure EVOH nanofibers. It was also worth noting that as the NaCoHCF content increases, the decomposition temperature decreases. This phenomenon can be attributed to several factors. One is the change in the thermal conductivity of the material. Because NaCoHCF is a metal complex, the EVOH/NaCoHCF nanofiber is expected to have higher thermal conductivity than the EVOH nanofiber. The temperature shown on the x-axis in Figure 4c is the programmed temperature for the measurement; however, the actual temperature inside the material may differ from this value depending on the thermal conductivity. Another reason is the change in the thermal stability and thermodynamics of the material. It is possible that the incorporated NaCoHCF altered the crystal structure and intermolecular forces between the polymer chains of EVOH, decreasing its thermal stability and thus inducing its thermal decomposition at a lower temperature. The presence of NaCoHCF in the nanofibers was confirmed by the NaCoHCF-derived behavior of the EVOH/NaCoHCF nanofibers.

As shown in Figure 4c, the final residual weight of the EVOH/NaCoHCF nanofibers increased as the NaCoHCF content in the electrospinning solution increased. The final residual weight is indicated by the light orange dotted line as raw data in Figure 4d, while the stronger orange color shows the actual NaCoHCF content in Figure 4d, calculated based on the TGA results. These values are close to the NaCoHCF content used in the preparation. The content of NaCoHCF in the EVOH/NaCoHCF nanofibers was calculated using the following equation (3):

$$Content\ of\ NaCoHCF\ in\ the\ nanofibers\ = W_{nanofibers} \times 100/W_{NaCoHCF} \quad (3)$$

where $W_{nanofibers}$ is the residual weight of each EVOH/NaCoHCF nanofibers at 550 °C, and $W_{NaCoHCF}$ is the residual weight of NaCoHCF powder at 550 °C, which is 59.9 wt%.

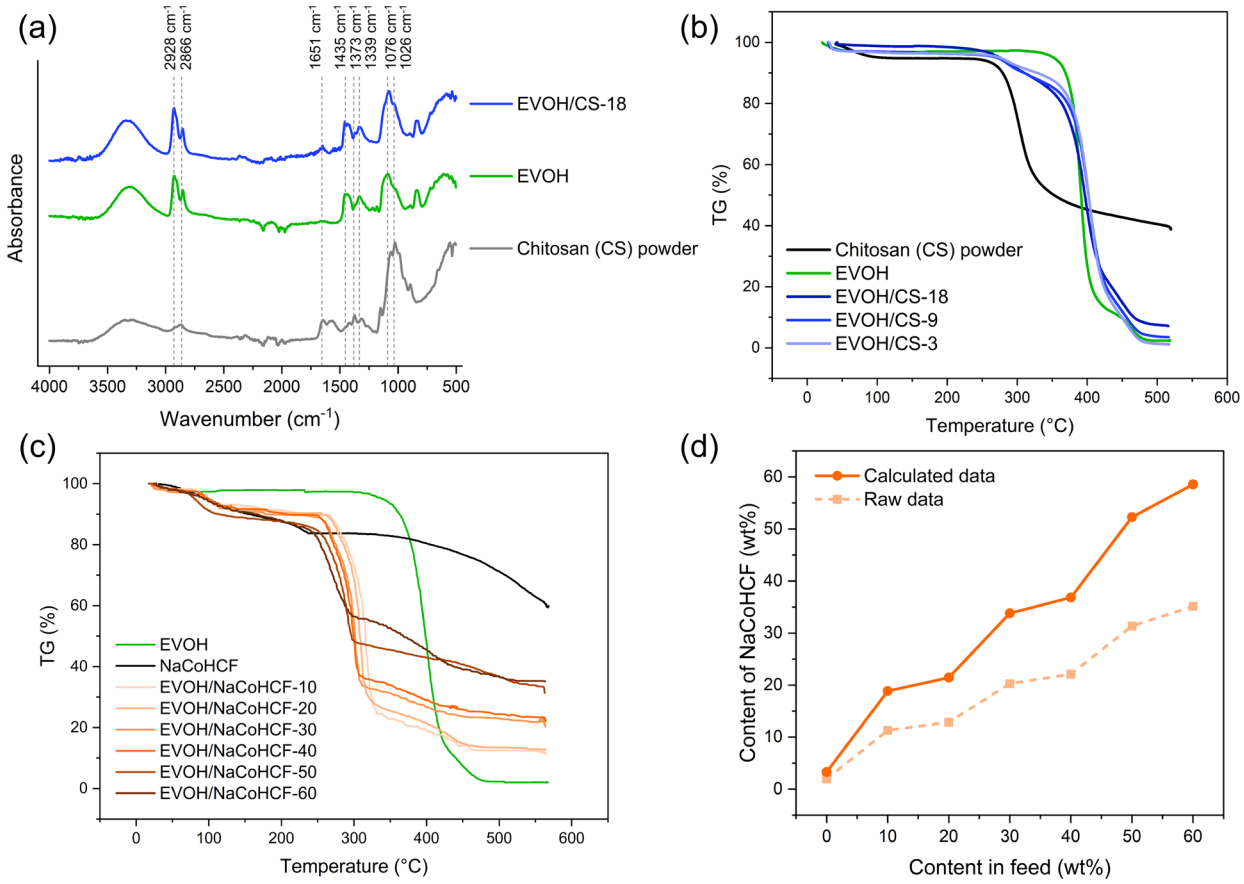

Figure 4. (a) FT-IR spectra and (b) TGA curves of chitosan, EVOH nanofibers, and EVOH/chitosan nanofibers. (c) TGA curves of the EVOH nanofibers, NaCoHCF powder, and EVOH/NaCoHCF nanofibers. (d) Residual mass and NaCoHCF content of EVOH/NaCoHCF nanofibers calculated via TGA.

3.5 Protein adsorption test of EVOH/chitosan nanofibers

Before applying the electrospun nanofibers in WAK, it is necessary to confirm their blood compatibility, because they will be in direct contact with blood. When albumin, a blood protein, is adsorbed and denatured on the surface of a material, platelet adhesion and activation are promoted, resulting in the formation of a thrombus. Therefore, protein adsorption is an important factor in evaluating the blood compatibility of a material. In general, a low protein adsorption level is desired.

In this study, the adsorption of HSA onto EVOH/chitosan nanofibers was evaluated. The HSA adsorption per unit weight of EVOH and EVOH/chitosan nanofibers is shown in Figure 5a. EVOH nanofibers adsorbed 3.87 μg/mg of HSA, and no significant difference was observed for EVOH/CS-3. However, HSA adsorption decreased significantly for the EVOH/chitosan nanofibers prepared with higher chitosan contents (EVOH/CS-9 and EVOH/CS-18), and the amount of adsorbed HSA was 0.20 μg/mg for EVOH/CS-18. To understand the cause of the significant reduction in protein adsorption, the surface wettability of the nanofibers with different chitosan contents was investigated through water contact angle measurements (Figure 5b). A surface is considered hydrophobic when the cosθ value of the water contact angle is less than 0 and hydrophilic when the cosθ value is greater than 0. As shown in Figure 5b, the EVOH nanofibers showed cosθ values between −0.3 and −0.5, indicating that they have a hydrophobic surface. In contrast, water droplets were absorbed by the surface of the EVOH/chitosan nanofibers after a few seconds of their placement, and the EVOH/chitosan nanofibers showed a cosθ value of 1.0 for the contact angle. This indicates that the addition of chitosan, which contains many amino and hydroxyl groups, to the EVOH nanofibers rendered the surface hydrophilic. In general, the adsorption of proteins, such as albumin, is less likely to occur on

hydrophilic surfaces. The obtained results suggest that the addition of chitosan rendered the EVOH/chitosan nanofiber surface hydrophilic and inhibited albumin adsorption.

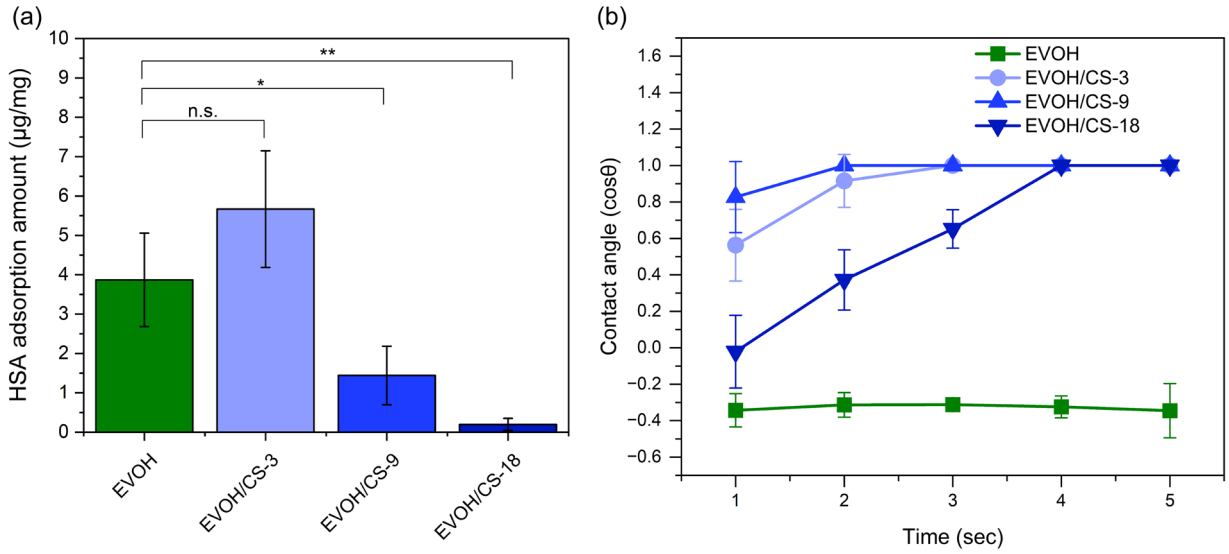

Figure 5. (a) Amount of HSA adsorbed by EVOH nanofibers and EVOH/chitosan nanofibers. (Mean ± SD, n = 3, *p < 0.05, **p < 0.01) (b) Change in the contact angle of a water droplet on the surfaces of EVOH nanofibers and EVOH/chitosan nanofibers over 5 s.

3.6 Evaluation of the urea degradation performance of urease-immobilized EVOH/chitosan nanofibers

Figure 6a shows the change in the urea concentration of urea-added PBS when the urease-immobilized EVOH nanofibers (EVOH@urease) and EVOH/chitosan nanofibers (EVOH/CS@urease) were used for urea degradation. The urea degradation rate of EVOH/CS@urease increased with increasing chitosan content. This may be attributed to the increased immobilization of urease in the nanofibers owing to the increased number of amino groups in the nanofibers at higher chitosan concentrations. The increase in the specific surface

area of the nanofibers may also have contributed to the increase in urease immobilization, because the fiber diameter decreased with the chitosan concentration, as shown in Figure 2b. EVOH/CS-18@urease degraded all urea within 1 h (the sample contained an urea concentration of 230 mg/dL typically found in CKD patients). Thus, the urea removal rate of EVOH/CS-18@urease was 690 mg/g per hour, which is higher than those reported for other materials (75.1-276.2 mg/g)[40–42]. The large specific surface area of the nanofibers is thought to be responsible for allowing more urease to come into contact with urea per hour. A decrease in urea concentration with urea removal rate of 402 mg/g per hour was also observed when EVOH@urease (without chitosan) were used. This is possibly because urease was immobilized via the reaction of glutaraldehyde with the hydroxyl groups of EVOH or by the physical adsorption of urease on the nanofibers. However, because the reactivity of hydroxyl groups with glutaraldehyde is much lower than that with amino groups and there is the risk of urease desorption when it is immobilized by physisorption, it is necessary to chemically crosslink it using the amino groups of chitosan.

To confirm the above hypothesis, urease was immobilized on two types of nanofibers and immobilization methods: EVOH nanofibers with glutaraldehyde (EVOH/GA), EVOH nanofibers without glutaraldehyde (EVOH), EVOH/chitosan nanofibers with glutaraldehyde (EVOH/CS/GA), and EVOH/chitosan nanofibers without glutaraldehyde (EVOH/CS). The changes in the urea removal performance during repeated urea degradation tests were evaluated (Figure 6b). The EVOH/chitosan nanofiber chemically crosslinked with glutaraldehyde (EVOH/CS/GA), shown in blue, retained 89% of its urea removal performance after six usage cycles. However, for the other three nanofibers, the urea removal performance gradually decreased with repeated use. Because these samples did not contain chitosan or glutaraldehyde,

or both, chemical crosslinking between urease and the nanofibers was not formed, and urease was probably immobilized via a weak reaction between the hydroxyl group of EVOH and glutaraldehyde or by physical adsorption, as described above. Nevertheless, because the immobilization of urease by these methods is not sufficiently stable, urease may have desorbed from the nanofibers during repeated use, resulting in a decline in the urea removal performance. If urease leaks into the bloodstream, changes in blood pH and excessive ammonium production occur; therefore, urease desorption is undesirable for the human body, and chemical crosslinking between the amino groups of chitosan and urease is necessary for its stable immobilization.

The urea degradation performance was also evaluated using real blood. EVOH/CS-18@urease chemically crosslinked with glutaraldehyde were immersed in whole porcine blood, and urea degradation was monitored. The changes in blood urea concentrations are shown in Figure 6c. The urea concentration changed similarly to that observed for PBS shown in Figure 6a, and almost all the urea in the blood was degraded in 60 min. Apart from urea, blood contains many other substances, such as electrolytes, proteins, and sugars. Therefore, when urea is removed by adsorption, selective urea adsorption is often inhibited by these substances, resulting in a significant decline in the urea adsorption performance of the adsorbent. However, our nanofibers could maintain high selectivity and urea removal performance for blood samples, because urease is an enzyme that specifically hydrolyzes urea.

The fiber morphology after urease immobilization was also observed by SEM (Figure S3a). The fiber shape was maintained even after urease immobilization, and it was confirmed that these nanofibers are stable.

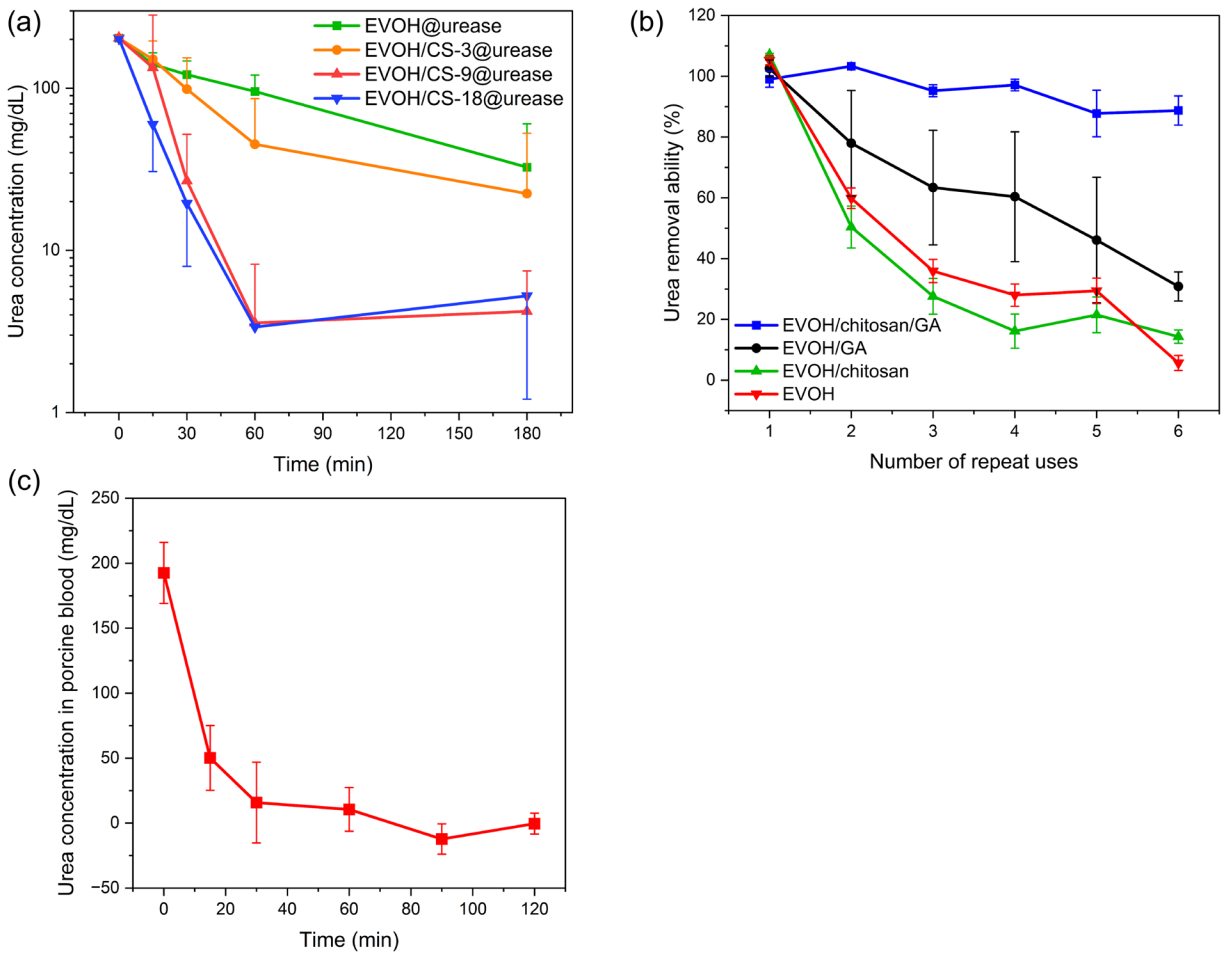

Figure 6. (a) Change in the urea concentration during urea decomposition tests using urease-immobilized EVOH nanofibers and urease-immobilized EVOH/chitosan nanofibers. (b) Change in the urea-removal capacity of different nanofibers with repeated use. (c) Change in the urea concentration of porcine blood during the urea decomposition test using EVOH/chitosan-0.7 nanofiber membrane with covalently immobilized urease. GA: glutaraldehyde.

3.7 Ammonium adsorption test using EVOH/NaCoHCF nanofibers

Figure 7a shows the results of the ammonium adsorption tests using the electrospun EVOH/NaCoHCF nanofibers. The gray plot represents the ammonium adsorption capacity of the

NaCoHCF powder, and the orange plot represents the ammonium adsorption capacity per gram of NaCoHCF in the EVOH/NaCoHCF nanofibers. The ammonium adsorption capacity of the NaCoHCF powder reached saturation in ~30 min, and 68.4 mg/g of ammonium was adsorbed after 2 h. However, for NaCoHCF in the EVOH/NaCoHCF nanofibers, the ammonium adsorption capacity was saturated in ~1 h. This may be due to the time required for the ammonium ions to diffuse through the EVOH layer covering the NaCoHCF particles. In this case, the amount of ammonium adsorbed after 2 h was 135.5 mg/g, which is approximately twice than that of the NaCoHCF powder. This can be attributed to several reasons, and one is related to the surface area of NaCoHCF. When NaCoHCF is used in water, the crystals form aggregates, which may lead to a decrease in the surface area. However, when NaCoHCF is loaded in the nanofibers, it is immobilized and does not aggregate, which increases the surface area and allows more ammonium to be adsorbed compared with that adsorbed in the powder state.

The XRD patterns of the NaCoHCF powder and EVOH/NaCoHCF nanofibers before and after ammonium adsorption are shown in Figure 7b. It has been reported that the crystal structure of the NaCoHCF changes following the adsorption of ammonium.[29] The broad peaks at approximately 25°, 40°, and 51° of the NaCoHCF crystals merged into a single sharp peak after ammonium adsorption, which is similar to the trend observed in previous studies. A similar peak change in the XRD pattern was also observed for the EVOH/NaCoHCF nanofibers, confirming that NaCoHCF in the nanofibers adsorbed ammonium.

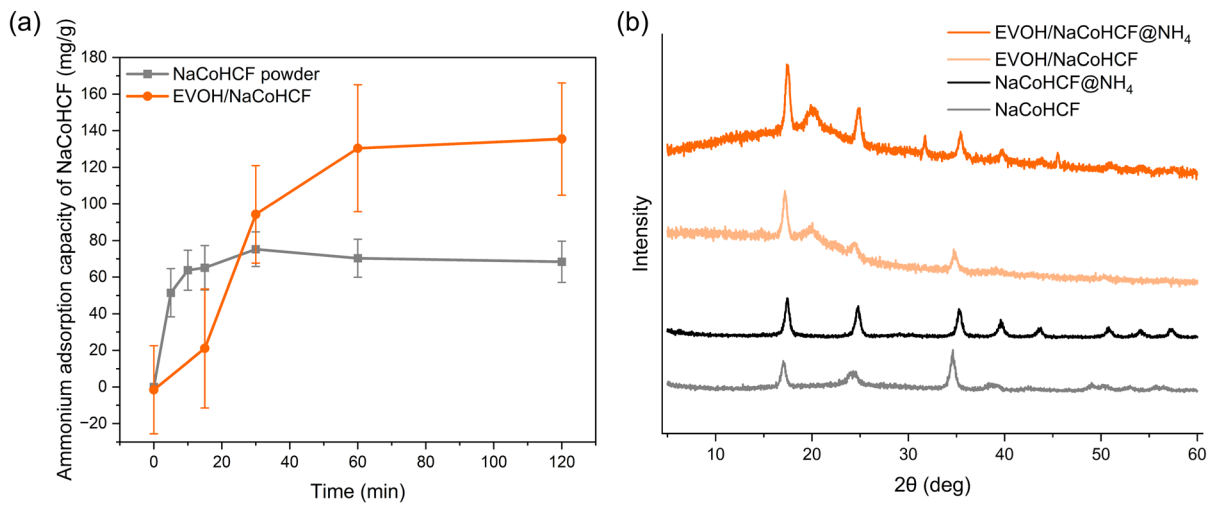

Figure 7. (a) Ammonium adsorption capacity of NaCoHCF in the powder state and in EVOH/NaCoHCF nanofibers. (b) XRD patterns of the NaCoHCF powder and EVOH/NaCoHCF nanofibers before and after ammonium adsorption (shown with "@NH_4" designation).

3.8 Fabrication of double-layered nanofibers and urea degradation test

Double-layered nanofibers were obtained by the sequential electrospinning of EVOH/chitosan and EVOH/NaCoHCF nanofibers, as described earlier. The FE-SEM images of the front and back sides of the double-layered nanofibers are shown in Figure 8a and Figure 8b, respectively. The successful fabrication of EVOH/chitosan and EVOH/NaCoHCF nanofibers in the double-layered nanofibers was confirmed by their similar appearance with the single EVOH/chitosan and EVOH/NaCoHCF nanofiber membranes. Figure 8c shows the cross-section of the double-layered nanofibers. The right and left sides show the EVOH/NaCoHCF and EVOH/chitosan nanofibers, respectively, with significantly different fiber diameters. The two nanofiber layers adhered and entangled well at the interface and did not easily separate. The SEM images of the morphology of double-layered nanofibers after urease immobilization are shown in Figure S3b

and Figure S3c. The both of front side and back side were stable and they kept their morphology even after urease immobilization.

Figure 8d shows the setup of the urea degradation test using the double-layered nanofibers. The ammonia measurement method employed within this work is not capable of measuring ammonia concentrations in blood, so the test was performed using an aqueous solution, not blood. The double-layered nanofiber membrane was placed in a filter holder connected to a diaphragm pump, and the urea solution (230 mg/dL, a concentration similar to that found in CKD patients)[11] was circulated through the membrane. The direction of the flow was from the front side to the back side of the double-layered nanofibers. Figure 8e shows the results of the urea degradation test. The red line shows the change in the urea concentration of the circulated solution, revealing that it decreased with time owing to the decomposition of urea. After 60 min of circulation, the urea concentration was successfully decreased to 23.0 mg/dL, which is within the standard blood urea concentration. The blue lines show the change in the ammonium concentration, and the solid and dotted lines represent the results for the double-layered nanofibers and EVOH/chitosan nanofibers (single-layer nanofibers membrane), respectively. Urea degradation by the urease-immobilized nanofibers produced ammonium, and the ammonium concentration in the solution after 4 h was 62.5 mg/dL for the EVOH/chitosan nanofibers, because the produced ammonium was not adsorbed. On the other hand, in the case of the double-layered nanofibers, the ammonium concentration in the solution increased immediately after the start of the test owing to urea degradation, and then it began to decrease owing to adsorption. The ammonium concentration in the solution after 4 h was 6.0 mg/dL. This result indicates that the ammonium produced due to urea degradation was adsorbed by NaCoHCF in the double-layered nanofibers. The final ammonium concentration was successfully reduced to approximately 10% of that

obtained with the single EVOH/chitosan nanofiber membrane. As ammonium in blood is toxic, even at small amounts, it is necessary to further reduce its concentration for practical application. This work, however, provides a proof of concept that both urea degradation and ammonium adsorption can be achieved with a single material.

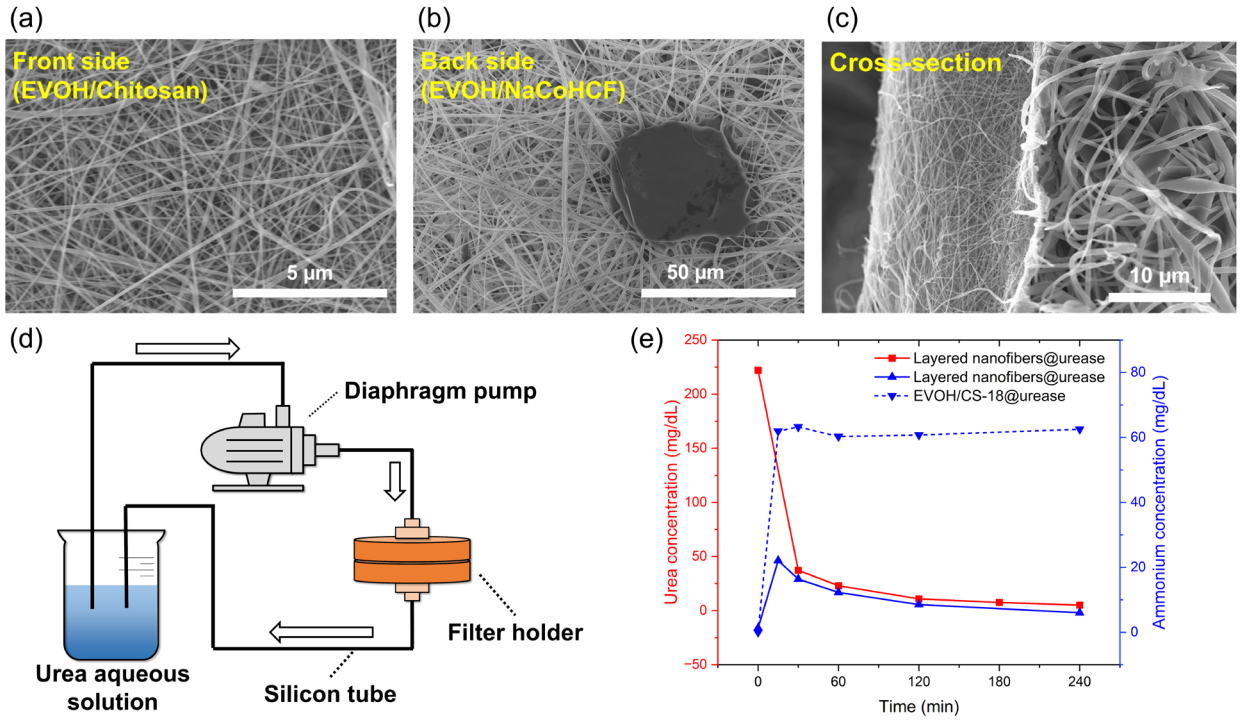

Figure 8. (a)–(c) FE-SEM images of the front side, back side, and cross-section of the double-layered nanofibers composed of EVOH/chitosan nanofibers and EVOH/NaCoHCF nanofibers. (d) Schematic illustration of the experimental setup used for the urea degradation test using double-layered nanofibers. (e) Change in urea and ammonium concentrations during urea decomposition tests using double-layered nanofibers. Blue triangles show the ammonium, while red dot shows the urea concentration.

4. Conclusion

To remove urea from the blood of patients suffering from CKD, urease was immobilized on EVOH/chitosan nanofibers fabricated by electrospinning. The urea degradation rate of the corresponding nanofibers increased with increasing chitosan content, the highest degradation rate was achieved by EVOH/CS-18@urease. The urease-immobilized EVOH/chitosan nanofibers exhibited a urea degradation rate of 690 mg/g per hour and thus efficiently decreased the urea concentration in the treated blood. In addition, chitosan not only helps urease immobilization through its free amine groups, it also improved hemocompatibility via suppressing protein adhesion. Further, EVOH nanofibers containing NaCoHCF, a metal complex, were prepared to remove the ammonium ions produced by urea degradation; the nanofibers were loaded with up to 50 wt% NaCoHCF. The NaCoHCF in the nanofibers showed a higher ammonium adsorption performance than that of the powdered sample, possibly because the electrospinning with EVOH prevented the aggregation of NaCoHCF particles and thus increased the effective surface area for ammonium adsorption. Finally, double-layered nanofiber membranes consisting of EVOH/chitosan (urease covalently immobilized) and EVOH/NaCoHCF nanofibers were fabricated and tested for urea degradation under continuous-flow circulating conditions. These membranes enabled the efficient reduction of both urea and ammonium concentrations. In the conventional degradation of urea in blood samples using urease, the production of highly toxic ammonium is problematic; however, the double-layered fiber material is capable of removing ammonium in addition to decomposing urea. The main advantage of this method compared to other urease immobilized mateirlas is that both urea and ammonium can be removed. Therefore, this material is expected to achieve highly efficient and safe removal of urea from blood, which is a major issue for the development of wearable artificial kidney, significantly accelerating the realization of such device as a game-changer in the treatment of chronic kidney disease.

ASSOCIATED CONTENT

Supporting Information.

The following files are available free of charge.

XRD pattern, EDX mapping, SEM images

AUTHOR INFORMATION

Corresponding Author

* Mitsuhiro Ebara – *Research Center for Macromolecules and Biomaterials, National Institute for Materials Science (NIMS), 1-1 Namiki, Tsukuba, Ibaraki 305-0044, Japan*

EBARA.Mitsuhiro@nims.go.jp

Present Addresses

† *Center for Advanced Materials, Forestry and Forest Products Research Institute, 1 Matsunosato, Tsukuba, Ibaraki 305-8687, Japan*

Author Contributions

The manuscript was written through contributions of all authors. All authors have given approval to the final version of the manuscript.

Funding Sources

JSPS KAKENHI Grant Number JP20H05877 and JP23KJ0260

Notes

ACKNOWLEDGMENT

This work was supported by JSPS KAKENHI Grant Number JP20H05877 and JP23KJ0260. A part of this work was supported by "Advanced Research Infrastructure for Materials and Nanotechnology in Japan (ARIM)" of the Ministry of Education, Culture, Sports, Science and Technology (MEXT).

ABBREVIATIONS

CKD, chronic kidney disease; WAK, wearable artificial kidney; EVOH, poly(ethylene-*co*-vinyl alcohol); FE-SEM, Field-emission scanning electron microscopy; FT-IR, Fourier transform infrared; HFIP, hexafluoro-2-propanol; XRD, X-ray diffraction; EVOH/CS, EVOH/chitosan nanofibers

REFERENCES

(1) Webster, A. C.; Nagler, E. V; Morton, R. L.; Masson, P. Chronic Kidney Disease. Lancet 2017, 389 (10075), 1238–1252. https://doi.org/10.1016/S0140-6736(16)32064-5.

(2) Bastani, B. The Present and Future of Transplant Organ Shortage: Some Potential Remedies. J. Nephrol. 2020, 33 (2), 277–288. https://doi.org/10.1007/s40620-019-00634-x.

(3) Sellarés, J.; De Freitas, D. G.; Mengel, M.; Reeve, J.; Einecke, G.; Sis, B.; Hidalgo, L. G.; Famulski, K.; Matas, A.; Halloran, P. F. Understanding the Causes of Kidney Transplant Failure: The Dominant Role of Antibody-Mediated Rejection and Nonadherence. Am. J. Transplant. 2012, 12 (2), 388–399. https://doi.org/10.1111/j.1600-6143.2011.03840.x.

(4) Hart, A.; Singh, D.; Brown, S. J.; Wang, J. H.; Kasiske, B. L. Incidence, Risk Factors, Treatment, and Consequences of Antibody‐mediated Kidney Transplant Rejection: A

Systematic Review. Clin. Transplant. 2021, 35 (7), e14320. https://doi.org/10.1111/ctr.14320.

(5) Ashuntantang, G.; Osafo, C.; Olowu, W. A.; Arogundade, F.; Niang, A.; Porter, J.; Naicker, S.; Luyckx, V. A. Outcomes in Adults and Children with End-Stage Kidney Disease Requiring Dialysis in Sub-Saharan Africa: A Systematic Review. Lancet Glob. Heal. 2017, 5 (4), e408–e417. https://doi.org/10.1016/S2214-109X(17)30057-8.

(6) Stephens, R. L.; Jacobsen, S. C.; Atkin-Thor, E.; Kolff, W. Portable/Wearable Artificial Kidney (WAK) - Initial Evaluation. Proc. Eur. Dial. Transpl. Assoc. 1976, 12, 511–518.

(7) Murisasco, A.; Baz, M.; Boobes, Y.; Bertocchio, P.; el Mehdi, M.; Durand, C.; Reynier, J. P.; Ragon, A. A Continuous Hemofiltration System Using Sorbents for Hemofiltrate Regeneration. Clin. Nephrol. 1986, 26 (Suppl 1), S53-7.

(8) Gura, V.; Beizai, M.; Ezon, C.; Polaschegg, H.-D. Continuous Renal Replacement Therapy for End-Stage Renal Disease. The Wearable Artificial Kidney (WAK). In Cardiovascular Disorders in Hemodialysis; KARGER: Basel, 2005; Vol. 149, pp 325–333. https://doi.org/10.1159/000085694.

(9) Gura, V.; Rivara, M. B.; Bieber, S.; Munshi, R.; Smith, N. C.; Linke, L.; Kundzins, J.; Beizai, M.; Ezon, C.; Kessler, L.; Himmelfarb, J. A Wearable Artificial Kidney for Patients with End-Stage Renal Disease. JCI Insight 2016, 1 (8), 1–15. https://doi.org/10.1172/jci.insight.86397.

(10) Davenport, A.; Gura, V.; Ronco, C.; Beizai, M.; Ezon, C.; Rambod, E. A Wearable Haemodialysis Device for Patients with End-Stage Renal Failure: A Pilot Study. Lancet 2007, 370 (9604), 2005–2010. https://doi.org/10.1016/S0140-6736(07)61864-9.

(11) Vanholder, R.; De Smet, R.; Glorieux, G.; Argilés, A.; Baurmeister, U.; Brunet, P.; Clark, W.; Cohen, G.; De Deyn, P. P.; Deppisch, R.; Descamps-Latscha, B.; Henle, T.; Jörres, A.; Lemke, H. D.; Massy, Z. A.; Passlick-Deetjen, J.; Rodriguez, M.; Stegmayr, B.; Stenvinkel, P.; Tetta, C.; Wanner, C.; Zidek, W.; EUTox. Review on Uremic Toxins: Classification, Concentration, and Interindividual Variability. Kidney Int. 2003, 63 (5), 1934–1943. https://doi.org/10.1046/j.1523-1755.2003.00924.x.

(12) D'Apolito, M.; Du, X.; Pisanelli, D.; Pettoello-Mantovani, M.; Campanozzi, A.; Giacco, F.; Maffione, A. B.; Colia, A. L.; Brownlee, M.; Giardino, I. Urea-Induced ROS Cause Endothelial Dysfunction in Chronic Renal Failure. Atherosclerosis 2015, 239 (2), 393–400. https://doi.org/10.1016/j.atherosclerosis.2015.01.034.

(13) D'Apolito, M.; Du, X.; Zong, H.; Catucci, A.; Maiuri, L.; Trivisano, T.; Pettoello-Mantovani, M.; Campanozzi, A.; Raia, V.; Pessin, J. E.; Brownlee, M.; Giardino, I. Urea-Induced ROS Generation Causes Insulin Resistance in Mice with Chronic Renal Failure. J. Clin. Invest. 2010, 120 (1), 203–213. https://doi.org/10.1172/JCI37672.

(14) van Gelder, M. K.; Jong, J. A. W.; Folkertsma, L.; Guo, Y.; Blüchel, C.; Verhaar, M. C.; Odijk, M.; van Nostrum, C. F.; Hennink, W. E.; Gerritsen, K. G. F. Urea Removal Strategies for Dialysate Regeneration in a Wearable Artificial Kidney. Biomaterials 2020, 234, 119735. https://doi.org/10.1016/j.biomaterials.2019.119735.

(15) Geremia, I.; A.W. Jong, J.; van Nostrum, C. F.; Hennink, W. E.; G.F. Gerritsen, K.; Stamatialis, D. New Mixed Matrix Membrane for the Removal of Urea from Dialysate Solution. Sep. Purif. Technol. 2021, 277 (15), 119408. https://doi.org/10.1016/j.seppur.2021.119408.

(16) Meng, F.; Seredych, M.; Chen, C.; Gura, V.; Mikhalovsky, S.; Sandeman, S.; Ingavle, G.; Ozulumba, T.; Miao, L.; Anasori, B.; Gogotsi, Y. MXene Sorbents for Removal of Urea from Dialysate: A Step toward the Wearable Artificial Kidney. ACS Nano 2018, 12 (10), 10518–10528. https://doi.org/10.1021/acsnano.8b06494.

(17) Liu, J.; Chen, X.; Shao, Z.; Zhou, P. Preparation and Characterization of Chitosan/Cu(II) Affinity Membrane for Urea Adsorption. J. Appl. Polym. Sci. 2003, 90 (4), 1108–1112. https://doi.org/10.1002/app.12841.

(18) Cheah, W. K.; Sim, Y. L.; Yeoh, F. Y. Amine-Functionalized Mesoporous Silica for Urea Adsorption. Mater. Chem. Phys. 2016, 175, 151–157. https://doi.org/10.1016/j.matchemphys.2016.03.007.

(19) Abidin, M. N. Z.; Goh, P. S.; Ismail, A. F.; Said, N.; Othman, M. H. D.; Hasbullah, H.; Abdullah, M. S.; Ng, B. C.; Kadir, S. H. S. A.; Kamal, F. Highly Adsorptive Oxidized Starch Nanoparticles for Efficient Urea Removal. Carbohydr. Polym. 2018, 201, 257–263. https://doi.org/10.1016/j.carbpol.2018.08.069.

(20) Kara, F.; Demirel, G.; Tümtürk, H. Immobilization of Urease by Using Chitosan–Alginate and Poly(Acrylamide-Co-Acrylic Acid)/κ-Carrageenan Supports. Bioprocess Biosyst. Eng. 2006, 29 (3), 207–211. https://doi.org/10.1007/s00449-006-0073-0.

(21) Zhang, J.; Yan, B.; He, C.; Hao, Y.; Sun, S.; Zhao, W.; Zhao, C. Urease-Immobilized Magnetic Graphene Oxide as a Safe and Effective Urea Removal Recyclable Nanocatalyst for Blood Purification. Ind. Eng. Chem. Res. 2020, 59 (19), 8955–8964. https://doi.org/10.1021/acs.iecr.0c00302.

(22) Talat, M.; Singh, A. K.; Srivastava, O. N. Optimization of Process Variables by Central Composite Design for the Immobilization of Urease Enzyme on Functionalized Gold Nanoparticles for Various Applications. Bioprocess Biosyst. Eng. 2011, 34 (6), 647–657. https://doi.org/10.1007/s00449-011-0514-2.

(23) Kutlu, N.; İspirli Doğaç, Y.; Deveci, İ.; Teke, M. Urease Immobilized Electrospun PVA/Chitosan Nanofibers with Improved Stability and Reusability Characteristics: An Application for Removal of Urea from Artificial Blood Serum. Prep. Biochem. Biotechnol. 2020, 50 (5), 425–437. https://doi.org/10.1080/10826068.2019.1679175.

(24) Kutcherlapati, S. N. R.; Yeole, N.; Jana, T. Urease Immobilized Polymer Hydrogel: Long-Term Stability and Enhancement of Enzymatic Activity. J. Colloid Interface Sci. 2016, 463, 164–172. https://doi.org/10.1016/j.jcis.2015.10.051.

(25) Hormozi Jangi, S. R.; Akhond, M. High Throughput Urease Immobilization onto a New Metal-Organic Framework Called Nanosized Electroactive Quasi-Coral-340 (NEQC-340) for Water Treatment and Safe Blood Cleaning. Process Biochem. 2021, 105, 79–90. https://doi.org/10.1016/j.procbio.2021.03.027.

(26) Ishii, Y.; Yarn, S.; Kanai, H.; Maezawa, A.; Tsuchida, A.; Wakamatsu, R.; Naruse, T. Evaluation of Blood Coagulation-Fibrinolysis System in Patients Receiving Chronic Hemodialysis. Nephron 1996, 73 (3), 407–412. https://doi.org/10.1159/000189101.

(27) Wang, J.; Zhuang, S. Chitosan-Based Materials: Preparation, Modification and Application. J. Clean. Prod. 2022, 355, 131825. https://doi.org/10.1016/j.jclepro.2022.131825.

(28) Aranaz, I.; Alcántara, A. R.; Civera, M. C.; Arias, C.; Elorza, B.; Caballero, A. H.; Acosta, N. Chitosan: An Overview of Its Properties and Applications. Polymers (Basel). 2021, 13 (19). https://doi.org/10.3390/polym13193256.

(29) Jiang, Y.; Minami, K.; Sakurai, K.; Takahashi, A.; Parajuli, D.; Lei, Z.; Zhang, Z.; Kawamoto, T. High-Capacity and Selective Ammonium Removal from Water Using Sodium Cobalt Hexacyanoferrate. RSC Adv. 2018, 8 (60), 34573–34581. https://doi.org/10.1039/C8RA07421F.

(30) Keirouz, A.; Wang, Z.; Reddy, V. S.; Nagy, Z. K.; Vass, P.; Buzgo, M.; Ramakrishna, S.; Radacsi, N. The History of Electrospinning: Past, Present, and Future Developments. Adv. Mater. Technol. 2023, 8 (11), 1–34. https://doi.org/10.1002/admt.202201723.

(31) Kobayashi, S.; Wakui, M.; Iwata, Y.; Tanaka, M. Poly(ω-Methoxyalkyl Acrylate)s: Nonthrombogenic Polymer Family with Tunable Protein Adsorption. Biomacromolecules 2017, 18 (12), 4214–4223. https://doi.org/10.1021/acs.biomac.7b01247.

(32) Cui, C.; Sun, S.; Wu, S.; Chen, S.; Ma, J.; Zhou, F. Electrospun Chitosan Nanofibers for Wound Healing Application. Eng. Regen. 2021, 2, 82–90. https://doi.org/10.1016/j.engreg.2021.08.001.

(33) Dodero, A.; Brunengo, E.; Alloisio, M; Sionkwoska, A.; Vicini, S.; Castellano, M. Chitosan-based Electrospun Membranes: Effects of Solution Viscosity, Coagulant and

Crosslinker. Carbohydr. Polym. 2020, 235, 115976, 1-8. https://doi.org/10.1016/j.carbpol.2020.115976

(34) Fong, H.; Chun, I.; Reneker, D. H. Beaded Nanofibers Formed during Electrospinning. Polymer 1999, 40 (16), 4585–4592. https://doi.org/10.1016/S0032-3861(99)00068-3.

(35) Lee, K. H.; Kim, H. Y.; Bang, H. J.; Jung, Y. H.; Lee, S. G. The Change of Bead Morphology Formed on Electrospun Polystyrene Fibers. Polymer 2003, 44 (14), 4029–4034. https://doi.org/10.1016/S0032-3861(03)00345-8.

(36) Sasaki, M.; Liu, Y.; Ebara, M. Zeolite Composite Nanofiber Mesh for Indoxyl Sulfate Adsorption toward Wearable Blood Purification Devices. Fibers 2021, 9 (6), 1–11. https://doi.org/10.3390/fib9060037.

(37) Aragón-Gutiérrez, A.; Heras-Mozos, R.; Gallur., M.; López, D.; Hernández-Muñoz., P. Hot-Melt-Extruded Active Films Prepared from Packaging Applications. Foods 2021, 10 (1591), 1–18.

(38) Yang, I.-H.; Szabó, L.; Sasaki, M.; Uto, K.; Henzie, J.; Lin, F.-H.; Samitsu, S.; Ebara, M. Biobased Chitosan-Derived Self-Nitrogen-Doped Porous Carbon Nanofibers Containing Nitrogen-Doped Zeolites for Efficient Removal of Uremic Toxins during Hemodialysis. Int. J. Biol. Macromol. 2023, 253 (3), 126880. https://doi.org/10.1016/j.ijbiomac.2023.126880.

(39) Zhang, N.; Kawamoto, T.; Jiang, Y.; Takahashi, A.; Ishizaki, M.; Asai, M.; Kurihara, M.; Zhang, Z.; Lei, Z.; Parajuli, D. Interpretation of the Role of Composition on the Inclusion

Efficiency of Monovalent Cations into Cobalt Hexacyanoferrate. Chem. - A Eur. J. 2019, 25 (23), 5950–5958. https://doi.org/10.1002/chem.201900097.

(40) Zhang, J.; Wang, Z.; He, C.; Liu, X.; Zhao, W.; Sun, S.; Zhao, C. Safe and Effective Removal of Urea by Urease-Immobilized, Carboxyl-Functionalized PES Beads with Good Reusability and Storage Stability. ACS Omega 2019, 4 (2), 2853–2862. https://doi.org/10.1021/acsomega.8b03287.

(41) Lv, M.; Ma, X.; Anderson, D. P.; Chang, P. R. Immobilization of Urease onto Cellulose Spheres for the Selective Removal of Urea. Cellulose 2018, 25 (1), 233–243. https://doi.org/10.1007/s10570-017-1592-3.

(42) Zhang, J.; Shi, Z.; He, C.; Song, X.; Yang, Y.; Sun, S.; Zhao, W.; Zhao, C. Urease Immobilized GO Core@shell Heparin-Mimicking Polymer Beads with Safe and Effective Urea Removal for Blood Purification. Int. J. Biol. Macromol. 2020, 156, 1503–1511. https://doi.org/10.1016/j.ijbiomac.2019.11.197.

TOC